Elastic Scattering of Protons at 31.5, 20, and 14.5 Mev

B. B. KINSEY* AND T. STONE†
Radiation Laboratory, University of California, Berkeley, California
(Received May 8, 1956)

A survey of the differential cross sections for the elastic scattering of protons has been made for protons of 31.5, 20, and 14.5 Mev. The angular distribution shows well-developed maxima and minima only for nuclei of intermediate atomic weight. For heavy nuclei, the diffraction effect is destroyed by the Coulomb scattering. With 31.5-Mev protons, the first minimum disappears for nuclei heavier than Zr; with 20-Mev protons, for nuclei heavier than V. In light nuclei, the maxima and minima are progressively obliterated as the mass number is reduced and the energy is increased. In the main, the angular distribution changes smoothly from one nucleus to another, the cross sections at the maxima increasing as the fourth power of the nuclear radius. However, these cross sections are not proportional to the energy, as would be expected from elementary diffraction theory. For intermediate nuclei, these cross sections are nearly independent of the energy; for nuclei from O to Mg they rise to a maximum near 20 Mev, and for light nuclei, they fluctuate in a less regular manner.

1. INTRODUCTION

THE angular distribution of elastically scattered protons was first reported by Burkig and Wright.[1] These authors measured the elastic scattering of 18.6-Mev protons from W, Pd, Ni, and Al. Further measurements were made subsequently by Gugelot,[2] using protons of a similar energy. At 22 Mev, the angular distribution was studied by Cohen and Neidigh[3] who showed that the positions of the maxima and minima of the diffraction pattern varied smoothly with atomic weight and were determined approximately by the product of the wave number and the nuclear radius. For protons of 30.6 Mev, accurate measurements have been made by Wright[4] for Be, C, and Al. More recently, measurements of the scattering of 31-Mev protons from carbon have been made by Hecht,[5] and from Al, Au, and Cu, by Leahy.[6] For protons of 20-Mev, extensive measurements have been made by Dayton and Schrank,[7] and Chow and Wright[8] have studied N and O. Finally, studies of the scattering of 10-Mev protons from C and Mg have been made by Fischer[9]; of 9.5-Mev protons from C and O by Burcham *et al.*,[10] and from N, Ne, and A by Freemantle *et al.*[11]

The measurements described here were made in order to extend the range of existing experimental data; to establish the general trends in the angular distribution as a function of both energy and atomic weight; and to make possible by theoretical analysis the determination of the magnitude of the nuclear potential and the other parameters of the complex potential model of the nucleus. In the present investigation, no attempt at precision has been made, for the work was intended only as a survey of elastic scattering. While the Rutherford scattering is the predominant process for high atomic weights and small angles of scattering, it will be shown that the characteristic maxima and minima of the nuclear scattering are displayed only by nuclei of intermediate atomic weight. For light elements, especially at the higher energies, these interference effects are largely destroyed, presumably, by the diffuse edge of the nucleus.[12]

2. EXPERIMENTAL

With slight modifications, the apparatus used in the present work was that described by Eisberg and Igo,[13] and the general procedure was similar to that described by Wright.[4] The arrangement is shown in Fig. 1. Measurements were made with the maximum energy proton beam from the linear accelerator (31.5 Mev), or with a beam of lower energy, *viz.*, 20 or 14.5 Mev, produced by retardation in plates of polystyrene. Three feet beyond the position of these absorbers, the beam was defined by passing it through a $\frac{3}{8}$-in. hole in a graphite block located at the entrance to a scattering chamber. Solid targets in the form of foils were placed at the center of the scattering chamber, which was evacuated by an auxiliary pumping system. Finally, the beam passed out of the scattering chamber through a thin window and entered an "integrator," a device in which the protons were stopped and the charge collected. The scattered protons were detected by a plastic scintillator and a photomultiplier enclosed in an air-tight box which could be rotated about the center of the scattering chamber by remote control. The

* Now at the Atomic Energy Research Establishment, Harwell, Berkshire, England.
† U. S. Navy, San Diego, California.
[1] J. W. Burkig and B. T. Wright, Phys. Rev. **82**, 451 (1951).
[2] P. C. Gugelot, Phys. Rev. **87**, 525 (1952).
[3] B. L. Cohen and R. V. Neidigh, Phys. Rev. **93**, 282 (1954).
[4] B. T. Wright, University of California Radiation Laboratory Report UCRL-2422, 1953 (unpublished).
[5] G. Hecht (to be published).
[6] J. Leahy (to be published).
[7] I. E. Dayton and G. Schrank, Phys. Rev. **101**, 1358 (1956).
[8] R. H. Chow and B. T. Wright, Phys. Rev. **99**, 640(A) (1955).
[9] G. R. Fischer, Phys. Rev. **96**, 704 (1954).
[10] Burcham, Gibson, Hossain, and Rotblat, Phys. Rev. **92**, 1266 (1953).
[11] Freemantle, Prowse, and Rotblat, Phys. Rev. **96**, 1268 (1954); Freemantle, Prowse, Hossain, and Rotblat, Phys. Rev. **96**, 1270 (1954).
[12] The author is indebted to Dr. W. Heckrotte for this suggestion, and for many valuable discussions.
[13] R. M. Eisberg and G. Igo, Phys. Rev. **93**, 1039 (1954).

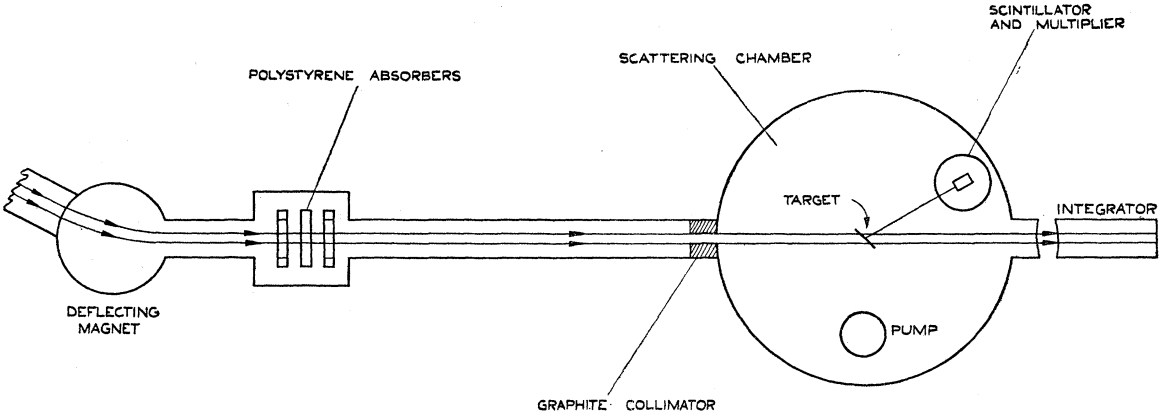

FIG. 1. General arrangement of apparatus.

scattered protons passed into the box through a thin aluminum window, the exposed area of the scintillator being defined by a $\frac{3}{8}$-in. square aperture cut in a $\frac{1}{4}$-in. aluminum plate. At 9 in. from the axis of the scattering chamber, this aperture subtended an angle of 3° at the axis. To study gases the scattering chamber was filled with the gas to be examined, the proton beam passing into it through a thin aluminum window.

When the sizes of the pulses produced by the scintillator are examined, the elastically scattered protons usually form a well-defined peak at the top end of the pulse-height spectrum. The remainder of the spectrum is caused by inelastically scattered protons. In the present apparatus the width of the peak (for 31.5-Mev protons) was about 4% of the height. Although this resolution was not always sufficient to separate entirely the inelastically scattered from the elastically scattered protons, the experimental errors which result from this incomplete separation are usually small. In the present apparatus the pulses from the scintillator were passed into a discriminator and then into a ten-channel pulse-height analyzer. Under normal working conditions one channel would count 75% of the elastically scattered protons. However, in practice, the discriminator was always adjusted so that the counting rate in the elastic peak was nearly equally divided between two adjacent channels. Such a procedure is convenient in that it is easy to adjust the discriminator quickly to satisfy this condition and, once adjusted, it is sufficient to record only the counts in the two adjacent channels.

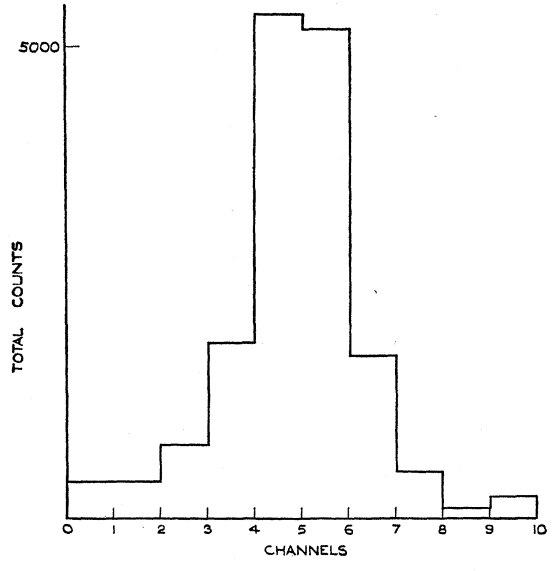

FIG. 2. Peak in pulse-height spectrum of 31.5-Mev protons scattered elastically from aluminum at 50°. The channels are 5 volts wide and the peak is at 80 volts.

A typical histogram is shown in Fig. 2. It is that produced by 31.5-Mev protons from the thin aluminum foil used for comparison purposes. Inspection shows a tail on the low-energy side of the elastic peak. This is caused by inelastically scattered protons. In some nuclei, e.g., in C^{12}, the energy of the first excited state is large enough for the proton group producing it to be clearly separated from the elastic peak in the pulse-height spectrum. But in most cases the energy resolution was not sufficient to resolve the elastic peak from that corresponding to the first excited state, and it was therefore impossible to eliminate the inelastic scattering entirely. However, unless the lowest excited states of the target nucleus are excited with exceptional frequency, or unless the elastic scattering itself is low, as at diffraction minima, or at high angles of scattering, then the contribution of inelastic scattering to the counting rate in the two adjacent channels is negligible. The total number of counts in the elastic peak is obtained by dividing the number of counts in the two adjacent channels by a factor, β, which represents the fraction of the peak recorded in the two channels. This fraction is calculated from the data of the pulse-height analysis on the assumption that the elastic peak would be symmetrical in shape were it not for the effect of the inelastically scattered protons. Thus, the total number of counts in the entire peak is calculated by adding to the counts recorded in the two adjacent channels,

twice the sum of the counts recorded in all higher channels (excepting only the last channel which records *all* pulses greater than those in the channels preceding it).

3. SOLID TARGETS

Metallic foils were mounted one vertically above another on a frame set at 45° to the proton beam. The target presented to the beam could be changed by raising or lowering the frame by remote control. An aluminum foil (12.0 mg cm^{-2}) mounted on the same frame served as a standard for comparison purposes.

Let q be the number of counts recorded in the two adjacent channels per unit charge; W, and A, the surface density and atomic weight of the target material, respectively; and let the subscript 0 refer to the quantities appropriate to the aluminum standard. Then the differential cross sections per unit solid angle are related by the equation

$$(d\sigma/d\Omega)/(d\sigma/d\Omega)_0=(q/q_0)(\beta_0/\beta)(AW_0/27W), \quad (1)$$

where β is defined in the previous section. This equation is valid only if the foils are thin enough to ensure that all the proton current is collected by the integrator. In the present apparatus, experiments with copper foils showed that there was no appreciable loss of proton current (for 31.5-Mev protons) provided that the foil was thinner than 75 mg cm^{-2}.

The experimental procedure was as follows. First, for 31.5-Mev protons, the number of counts per unit charge from the aluminum standard was measured at a scattering angle of 50°. (There is a maximum in the diffraction pattern of aluminum at 50° and at this angle, therefore, the number of counts was nearly independent of small errors in the angular setting of the detector.) Second, the proton energy having been adjusted to the appropriate value, the number of counts per unit charge was measured at different angles to the target to be studied. Finally, the proton energy being put back to 31.5 Mev, the number of counts from the aluminum standard was remeasured at 50°.

These measurements, together with the weights of the foils, and measurements of β, determine the ratio of the differential cross sections. The absolute value was obtained when the magnitude of the charge, the angle of the target to the proton beam, and the aperture of the scintillator are taken into account. For aluminum the average of a number of measurements of the cross section at 50° and at 31.5 Mev was 50 mb per steradian, in agreement with the value (55 mb) determined by Leahy[6] with similar apparatus but different geometry and different methods of detection. The accuracy was about 10%.

Apart from the energy difference between the incident and scattered proton, which is caused by the recoil of the target nucleus, the energy of the scattered proton depends on the depth at which it originates in the target. The arrangement of the target relative to the detector for small angles is shown in Fig. 3(a). In this case the energy difference between the protons scattered at opposite surfaces of the target is very small: it is equal to the difference in the energies lost by the proton beam in traversing thicknesses equal to OA and OB in the target. The width of the peak, then, is that caused by the characteristics of the scintillator; it is constant for protons of a given energy, and, within wide limits, it is independent of the thickness and composition of the target. For protons of the same energy, the two values of β in Eq. (1) are equal (at 31 Mev, $\beta\sim0.75$). For decreasing energies, β increases at first, and then falls.

For large angles, the protons must be detected at the near side of the target [Fig. 3(b)]. In this case the protons scattered from the surface of the target facing the beam lose no energy other than that due to recoil, while those scattered at the far surface lose, in addition, an amount which (for a target at 45° to the beam) is never less than 2.4 times the energy loss in transmission at normal incidence. Therefore, unless very thin targets are used, the width of the peak is increased above the natural width due to the scintillator, and its position is displaced towards lower energies. Thus, the comparison of cross sections now always involves two measurements of β. At high angles, the counting rates are very low, and it is very difficult to avoid this additional source of error.

For materials obtainable only in powdered form, e.g.,

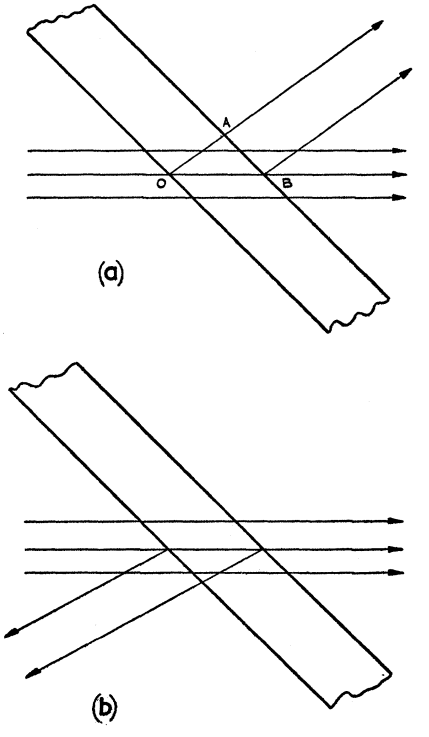

FIG. 3. Protons scattered in forward direction (a) have very nearly the same energy; those scattered in backward direction (b) differ by at least 2.4 times the retardation in normal transmission through the target.

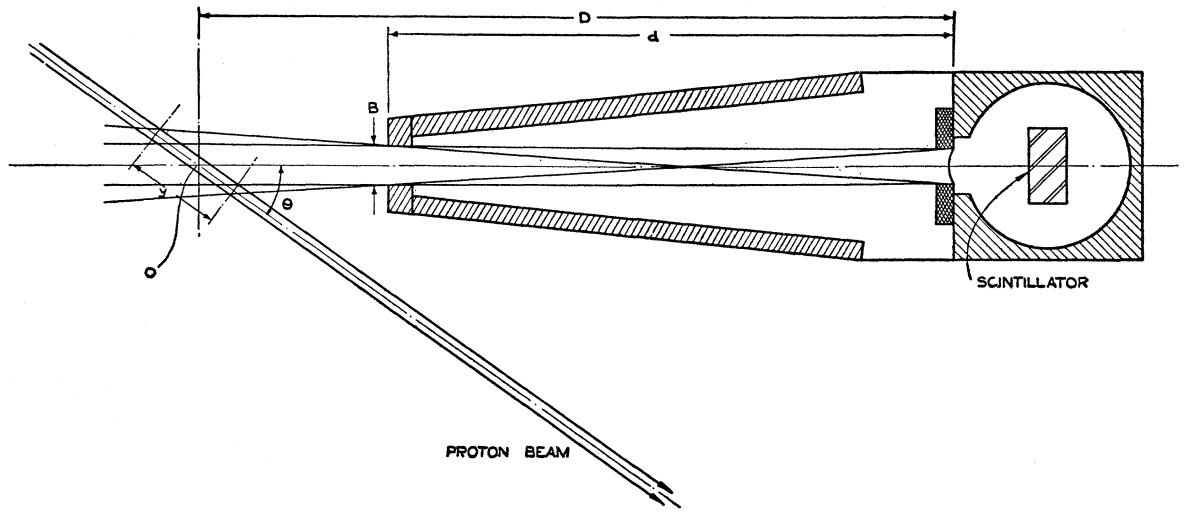

FIG. 4. Arrangement for studies of scattering in gases.

B, P, and Si, self-supporting foils, usually about 20 mg cm^{-2}, were made by sedimentation in water mixed with a little glue to give adhesion. The material, which was deposited on a glass plate, was dried, coated with plastic spray to give further adhesion, and then stripped off, cut, and weighed.[14] Generally, the measurements made with such foils were less accurate than those obtained with metallic foils, and the additional error was about 5%.

Another source of error derived from counting rate losses: it was found that, if the average counting rate in the elastic peak is increased, the superposition of small background pulses on those produced by elastically scattered protons, broadened the peak, and shifted its centroid in the direction of higher energies. Thus, q, the counting rate in the adjacent channels, and β were reduced. All measurements, therefore, were made with a counting rate per channel of less than 500 per minute; for this rate the loss was empirically determined as 10%.

[14] The authors are much indebted to Mr. Herbert Robinson and Mrs. Potter for instruction and advice in the preparation of these foils. The weight of material deposited with the spray (usually about 0.5 mg cm^{-2}) was estimated from that deposited simultaneously on an adjacent metal foil. Several foils were made from each element and the number of protons per unit charge scattered at the first maximum of the diffraction pattern were compared. The consistency of these measurements left much to be desired; for example, the counting rates when divided by the thickness of the foil, would vary from one foil to another by about 10%. The angular distributions, therefore, were measured with one foil, the carbon contribution subtracted from it, and the results normalized using the average yield per unit thickness at the diffraction maximum. Attempts to prepare self-supporting foils of S in this way were a failure; only one successful foil was made on aluminum backing. The S results quoted below are a mean of the results obtained with this one foil and that found from carbon disulfide vapor. Foils of heavier elements (e.g., As), whether backed or self-supporting, were useless because of the large contribution of scattering by the unwanted light element at low scattering angles.

4. GASEOUS TARGETS

Some elements are not easily available as solids, and when present in compounds are combined with unwanted elements. Of these, N, O, and A, are best studied as pure gases, and chlorine, as the vapor of carbon tetrachloride.

For these measurements the scattering chamber was filled with the gas to be investigated, the proton beam entering the scattering chamber through a thin aluminum window and a graphite collimator. To limit the volume of the gas from which protons were scattered to

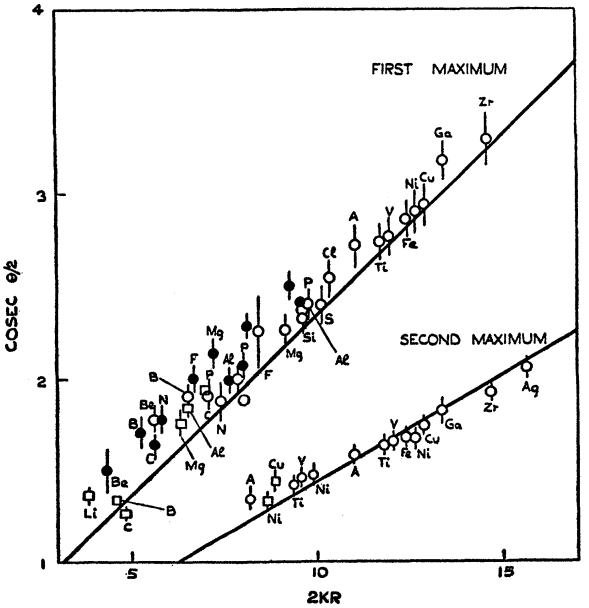

FIG. 5. Angles (θ) of first and second maxima. The wave number, k, is calculated for the center-of-mass system, $R=1.35A^{\frac{1}{3}}\times10^{-13}$ cm. The straight lines represent the equations: $2k(R+\lambda\!\!\!^{-})=5.2\csc(\theta/2)$ and $2k(R+\lambda\!\!\!^{-})=8.4\csc(\theta/2)$. Open circles, 31.5 Mev; full circles 20 Mev; squares 14.5 Mev.

the scintillator, an aluminum mask was fitted to the scintillator. With this arrangement (Fig. 4) the following procedure was adopted.

(a) First, the scattering chamber was filled to atmospheric pressure with the gas to be examined, and the elastically scattered protons were counted at different angles. These measurements, corrected by multiplying each count by the sine of the scattering angle, determine only the relative angular distribution, since multiple scattering of the proton beam within the chamber reduced the proton current collected at the integrator by an indeterminate amount.

(b) Second, at a much lower pressure,[15] the scattering at a maximum in the diffraction pattern found in (a) was measured and compared, after evacuation of the chamber, with that obtained from the standard aluminum sample. For this comparison, it was essential that all parts of the aluminum standard which were exposed to the beam should have an unimpeded view of the scintillator. In the present apparatus, this condition was obtained when the area of the beam was reduced to a ribbon, $\frac{3}{8}\times\frac{1}{8}$ in., with its longer axis perpendicular to the rotation of the scintillator.

The absolute value of the differential cross section at various angles was found by combining the two sets of measurements. Let q be the number of counts recorded per unit charge at a diffraction maximum; y, the effective thickness of the gas exposed to the view of the scintillator; ρ, the density; n, the number of atoms per molecule; M, the molecular weight; and let the subscript, 0, as before, refer to the aluminum standard. Then the measurement (b) gives

$$q/q_0=[(d\sigma/d\Omega)\beta n\rho y/M]/[(d\sigma/d\Omega)_0\beta_0 W_0 \csc 45°/27]. \quad (2)$$

Provided that the scattering angle is not too small, the effective length, y, may be obtained by calculation.[16] To check the validity of such a calculation, y was also determined experimentally by measuring the ratio (R) of the counting rate produced by acetylene (density ρ_a) to the counting rate from a polystyrene foil (surface density W) set at 45° to the beam. Then $y=RW \csc 45°/\rho_a$. The calculated and experimental values of y were in good agreement, except at high angles where the very low counting rates caused by acetylene were difficult to measure, and at low angles, below 30°, where y is no longer strictly proportional to $\csc\theta$.

For the calibration of gaseous targets against the aluminum standard [measurement (b) above], the counting rates were very low and consequently the maximum beam current was used. The background of small pulses was high and therefore the elastic peak, superposed on this background, was wider than usual. The errors in absolute measurements with gaseous targets were probably about 15%.

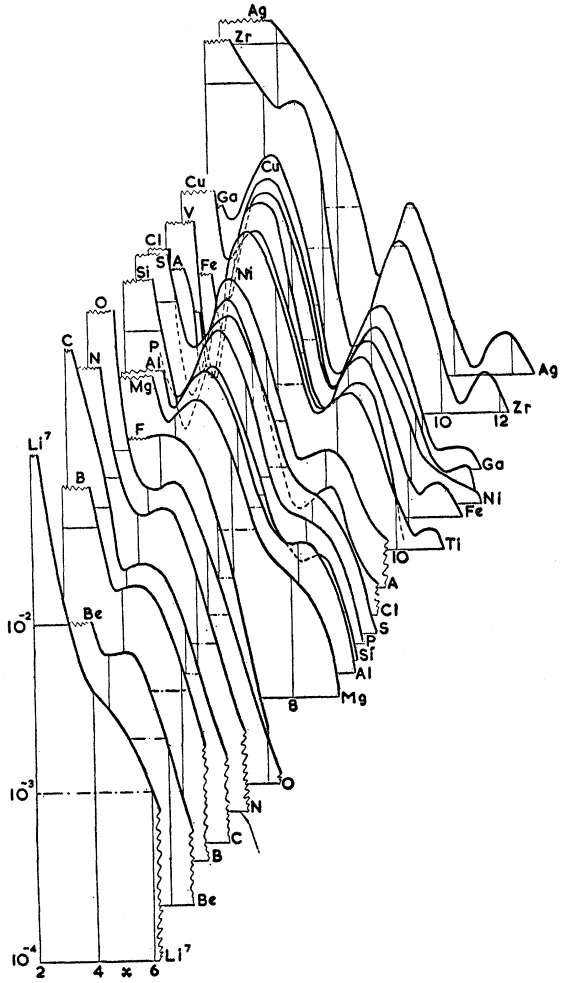

FIG. 6. Differential cross sections, in units of $k^2R'^4$, plotted against x, for 31.5-Mev protons.

5. RESULTS

In agreement with the findings of Cohen and Neidigh,[3] the present investigation shows that the maxima and minima occur approximately at the angles predicted by the elementary theory of diffraction. According to this, the differential cross section is given by[17,18]

$$d\sigma/d\Omega=k^2R'^4[J_1(x)/x]^2, \quad (3)$$

where $x=2kR'\sin(\theta/2)$; R' is the sum of the nuclear radius and the wavelength, $R'=R+\lambda\!\!\!^{-}$; and k is the wave number, calculated for the center-of-mass system.

[15] The counting rates were compared for that maximum gas pressure for which experiment showed that there was no appreciable loss of beam current at the integrator.

[16] For a rectangular aperture before the scintillator, and for a defining slit (width B), with its vertical edges parallel to that of the aperture, the effective length is $y=BD/d$. $\csc\theta$, where D and d are the distances from the aperture to the axis of rotation (assuming that the beam passes symmetrically through it) and from the aperture to the slit (Fig. 4), respectively.

[17] G. Placzek and H. Bethe, Phys. Rev. **57**, 1075(A) (1940).

[18] A. Akhieser and I. Pomeranchuk, J. Phys. (U.S.S.R.) **9**, 471 (1945).

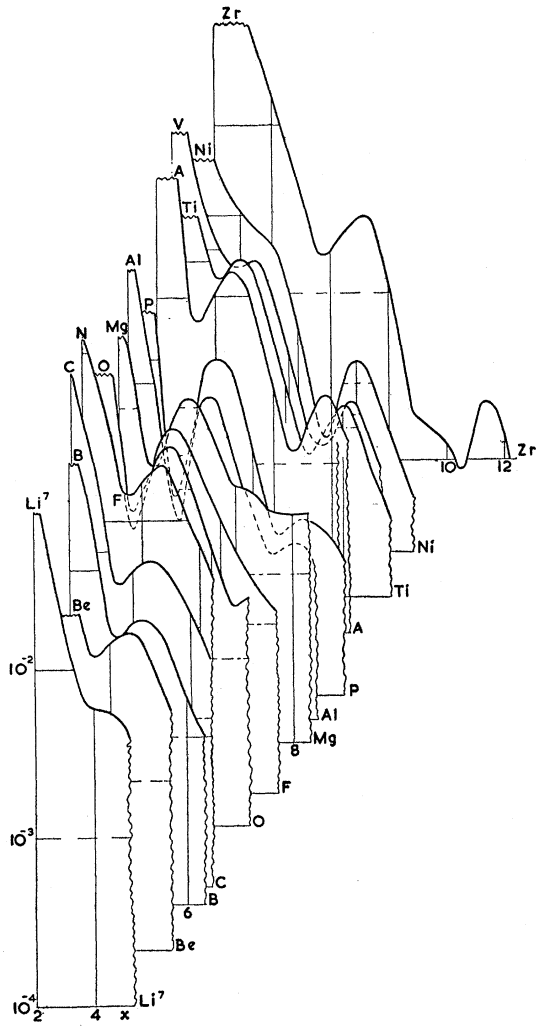

FIG. 7. Differential cross sections, in units of $k^2R'^4$, plotted against x, for 20-Mev protons.

Minima occur when $J_1(x)=0$, i.e., when $x=3.8$, 7.0, etc., and maxima for $x=5.2$, 8.4, etc. In Fig. 5, the cosecants of the experimentally determined half-angles for the first and second maxima are plotted against $2kR$, with $R=1.35A^{\frac{1}{3}}\times10^{-13}$ cm. The straight lines represent the predicted positions of the maxima. It will be seen that there is good agreement. This is quite remarkable in view of the crudity of the model.

There is, however, only fair agreement between the cross sections predicted by (3) and those obtained experimentally. For the second maximum, where this is developed (from A to Ag for 31-Mev protons) the agreement is good (to 10%). But for the first maximum, for protons of this energy, the experimental cross sections are too large by a factor of 2. Furthermore, the expression (3) predicts that the cross sections should fall to zero at the minima. Experimentally, making allowances for finite resolution, the cross sections at the first minimum never fall much below one tenth of that at the first maximum.

The general trends of the cross sections are shown in Figs. 6, 7, and 8. Here, the differential cross sections, in units of $k^2R'^4$, are plotted against the parameter x. For 31.5-Mev protons, the contrast between the cross sections at minimum and at maximum is greatest at V^{51}. For lower proton energies, the diffraction effects are less obvious: the first minimum, which is at its greatest depth in V^{51}, for 31.5-Mev protons, has all but disappeared at 20 Mev. The contrast is reduced as the mass number is reduced. For 31.5-Mev protons, diffraction effects have disappeared altogether in Li^7. For the lightest nuclei, however, they reappear as the proton energy is reduced.

It is clear that for the higher energy protons, for given values of x, the cross sections are proportional to R'^4 and vary rather smoothly from one element to another. This smooth variation is shown in Fig. 9 where the

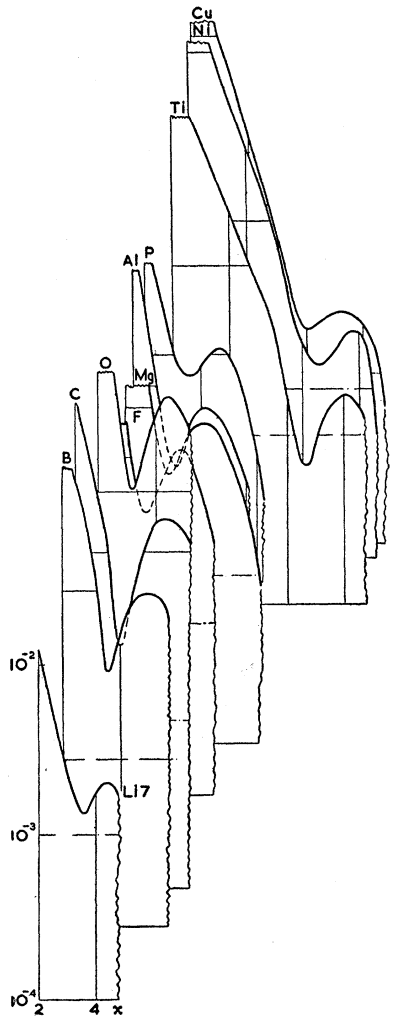

FIG. 8. Differential cross sections, in units of $k^2R'^4$, plotted against x, for 14.5-Mev protons.

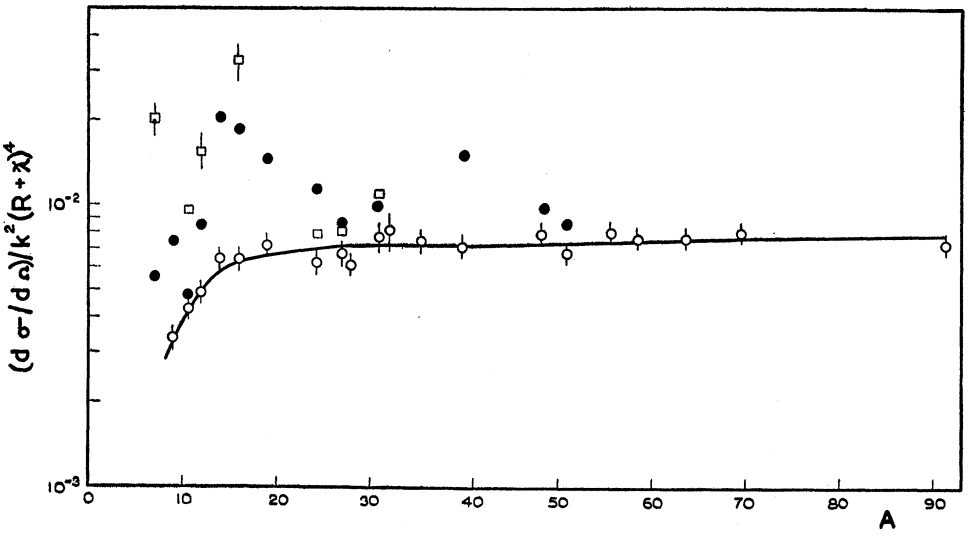

FIG. 9. Differential cross section at the first maximum, in units of $k^2R'^4$, plotted against atomic weight, A. Open circles: 31.5 Mev; full circles, 20 Mev; squares, 14.5 Mev.

cross sections for the first maximum, in units of $k^2R'^4$, are plotted against the atomic weight. For decreasing mass numbers, the cross sections, measured in these units, decrease as the diffraction phenomenon disappears. For lower energy protons, the variation in cross sections is less smooth, and for some light nuclei, the cross sections are quite erratic.

According to (3), the cross sections at the maxima should fall linearly with the proton energy. This does not occur. For $A\sim50$, the cross section at the first maximum appears to be nearly independent of proton energy. For lighter nuclei ($A\sim20$), the cross section reaches a maximum near 20 Mev. This effect is quite marked for F and Mg, but has disappeared at Al. For decreasing mass numbers the energy at which this cross section is a maximum decreases. The effect is shown clearly in Figs. 10 to 13.

6. CONCLUSIONS

The smooth variation of the differential cross section in intermediate nuclei can be ascribed to regular changes

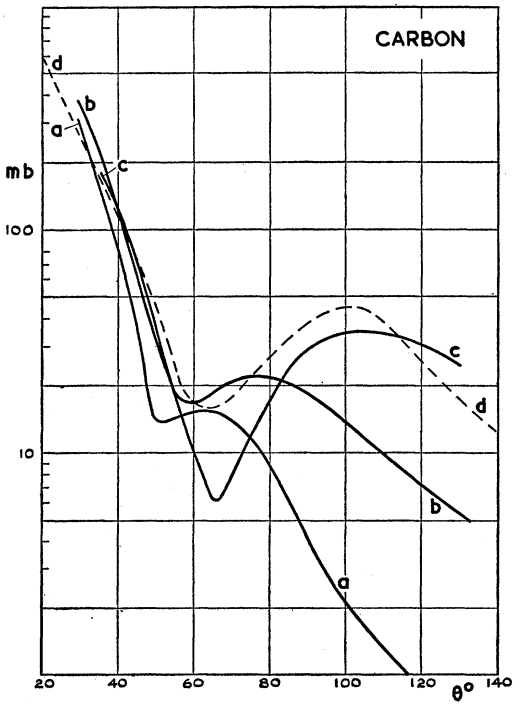

FIG. 10. Differential cross sections for carbon in mb per steradian. (a) 31.5 Mev; (b) 20 Mev; (c) 14.5 Mev; (d) 9.5 Mev according to Burcham, Gibson, Hossain, and Rotblat.[10]

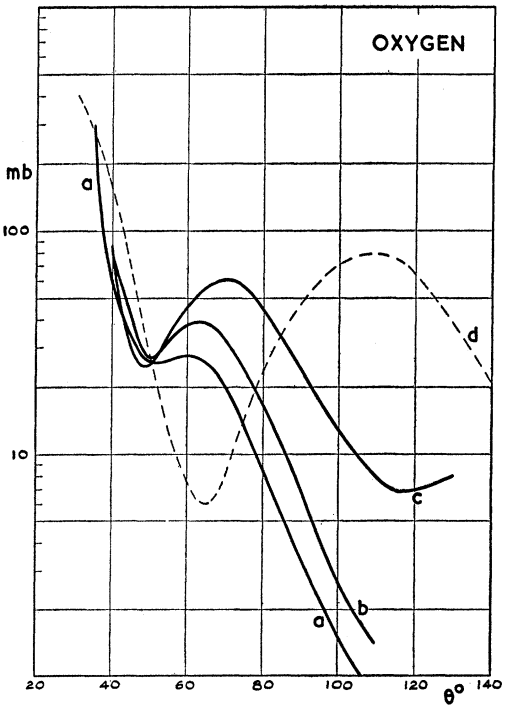

FIG. 11. Differential cross sections for oxygen, in mb per steradian. (a) 30.4 Mev; (b) 24.3 Mev; (c) 18.5 Mev; (d) 9.5 Mev according to Burcham, Gibson, Hossain, and Rotblat.[10]

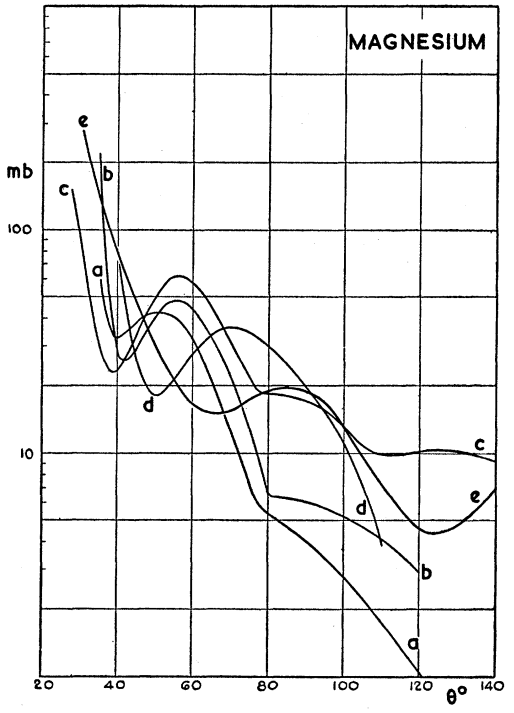

FIG. 12. Differential cross sections for magnesium in mb per steradian (a) 31.5 Mev; (b) 25.4 Mev; (c) 20 Mev; (d) 14.5 Mev; (e) 10.0 Mev according to Fischer.[9]

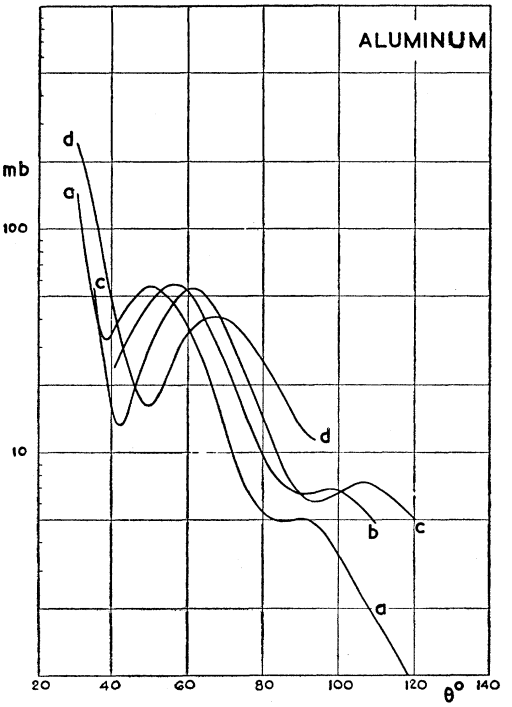

FIG. 13. Differential cross sections for aluminum in mb per steradian. (a) 31.5 Mev; (b) 25.4 Mev; (c) 20 Mev; (d) 14.5 Mev.

in nuclear properties and to the fact that a relatively large number of proton waves of different angular momenta must contribute to the elastic scattering. The smaller number of partial waves for light nuclei, and the relatively greater importance of any one of them, is no doubt responsible for the less regular behavior in light nuclei. In broad outline the results described here have been satisfactorily accounted for by Saxon and his associates,[19] who have determined the parameters of the complex potential model which give a best fit to the experimental results. The most important of these is the depth of the potential well for 31.5-Mev protons, which is less deep than that which obtains for low-energy neutrons, and the taper of the well, which seems to account satisfactorily for the obliteration of the diffraction effects at high energies in light nuclei.

[19] D. Saxon (to be published).

ACKNOWLEDGMENTS

The authors wish to thank Dr. Finke for suggesting the use of plastic scintillators in these measurements, and for much assistance in setting up the apparatus, especially in its early stages; Dr. Heckrotte and Dr. Saxon for theoretical advice; Mr. Robert Watt and the staff of the linear accelerator for their generous assistance; and finally Professor Ernest O. Lawrence for the privilege of working at the Radiation Laboratory.